Lattice-dynamical effects and hyperfine interactions in Cu-Zn alloys

M. Peter, W. Potzel, M. Steiner, C. Schäfer, H. Karzel, W. Schiessl, and G. M. Kalvius
Physik-Department E15, Technische Universität München, D-8046 Garching, Germany

U. Gonser
Grundlagen der Materialkunde, Universität des Saarlandes, D-6600 Saarbrücken, Germany
(Received 18 May 1992)

The temperature dependence of lattice-dynamical effects has been investigated between 4.2 and 60 K in Cu-Zn alloys containing 15.9 at. % Zn (α-phase) and 49.2 at. % Zn (β'-phase). A comparison of the 93.31-keV ^{67}Zn Mössbauer data on the Lamb-Mössbauer factor (LMF) and on the second-order Doppler effect (SOD) for both structures as well as low-temperature x-ray experiments show that no β'-phase exists in the α-alloy contrary to the prediction of a hypothetical phase diagram proposed recently. The LMF and SOD decrease drastically with increasing temperature. The temperature variations of the LMF and SOD of both alloys are in good agreement with the results of model calculations of interatomic force constants based on phonon dispersion relations which were derived from inelastic neutron scattering data.

I. INTRODUCTION

The Cu-Zn alloy system (brass) has been of enormous technological and theoretical interest because of the rich phase diagram[1] that is the prototypical representative of a class of alloys known as Hume-Rothery alloys.[2–4] For this class of materials it has been emphasized that phase stability properties are driven by the average concentration of conduction electrons, or electron to atom ratio (Hume-Rothery rules). Hence these alloys have also been called "electron phases." More recent Mössbauer investigations have demonstrated that in the α-phase (fcc-structure) short-range order is present, which leads to only four different Cu-Zn configurations instead of the expected binomial distribution of Zn in Cu.[5,6] The ability of α-brass, with composition around Cu_3Zn, to form long-period superstructures as suggested by short-range-order diffuse scattering intensity in neutron diffraction experiments[7] was also revealed by first-principle phase stability calculations.[8]

Dilatometry and electron microscopy on a β-alloy (with ~60% Cu) which was aged for ~30 years suggested, however, that the phase diagram might have to be revised.[9] In particular, in the low-temperature regime, the region of the β- and β'-phases might have to be extended considerably towards lower Zn concentration at the expense of the α-phase. Into the same line of reasoning fitted the results of high-pressure Mössbauer experiments, which showed that, surprisingly, the center shift (CS) of one of the four Cu-Zn configurations of the α-phase decreased by the same amount as the CS of the β'-phase when the volume of the unit cell is reduced.[6]

To help to clarify these questions of phase stability at low temperatures we report on Mössbauer transmission experiments on Cu-Zn alloys containing 15.9 at.% Zn (α-phase) and 49.2 at.% Zn (β'-phase) in the temperature range between 4.2 and 60 K. We investigated temperature-dependent lattice-dynamical effects (Lamb-Mössbauer factor and second-order Doppler shift) as well as the isomer shift in these alloys. In addition, we performed x-ray diffraction experiments on the same alloys between ~10 K and room temperature. Our results show that in our sample of α-brass which was aged for ~10 years at room temperature all four Cu-Zn configurations belong to the α-phase and that no β'-phase is present.

II. EXPERIMENTAL DETAILS

Mössbauer measurements were carried out in transmission geometry using a piezoelectric quartz spectrometer. Its design, including the modifications for heating the absorber and the calibration of the small Doppler velocities, have been described in previous publications.[10,11]

As Mössbauer sources we used ^{67}Ga in Cu metal, which exhibits a single Lorentzian line. The ^{67}Ga (half-life of $T_{1/2}$=78 h) activity was produced *in situ* by 46-MeV α-bombardment of Cu disks with natural abundance of the Cu isotopes. The disks were 8 mm in diameter and 0.5 mm in thickness. The irradiations were carried out at the cyclotron of the Kernforschungszentrum Karlsruhe. The sources were used without annealing about 48 h after the end of irradiation.[6]

The brass absorbers were prepared from high-purity copper and from zinc metal enriched to ~91% in ^{67}Zn. The zinc concentration was 15.9 at.% (α-phase) and 49.2 at.% (β'-phase); disks with ~8 mm diameter were used with absorber thicknesses of 0.194 and 0.530 g/cm^2 of ^{67}Zn, respectively. For the 60 K measurement the thickness of the α-absorber was increased to 0.382 g/cm^2 of ^{67}Zn. The disks were cut without cold-working from a larger ingot. Further details are given in Ref. 6. An intrinsic Ge detector coupled to fast pulse-counting elec-

tronics allowed count rates up to 120 000 s^{-1} in the 93.31-keV window with a signal-to-background ratio of S/(S+B)~0.60.[12]

X-ray diffraction measurements at ambient pressure were performed on the same alloys in the temperature range between 10.6 and 304 K. The powder samples were filed from the Mössbauer absorbers and fixed between two pieces of cellophane tape. They had a diameter of 3 mm and a thickness of ~27 mg/cm^2. In addition, the lattice constants at room temperature were determined for the alloys with 4.3 at.% Zn and 42.8 at.% Zn in Cu. The Guinier-type diffractometer, which includes a liquid-He cryostat, has been described earlier.[13,14]

III. RESULTS

A. Mössbauer measurements

Figure 1 displays Mössbauer absorption spectra of the α-phase alloy recorded between 4.2 and 60 K. These spectra were fitted by a superposition of four independent Lorentzian lines.[6] Figure 2 shows absorption spectra of the β'-phase. At all temperatures investigated the β'-absorber exhibits only a single absorption line. The results are summarized in Tables I and II. The temperature dependences of the Lamb-Mössbauer factor (LMF) as derived from the total area under the absorption lines, of the mean-square atomic displacement $\langle x^2 \rangle$ and of the center shift (relative to 4.2 K) are given in Tables III and IV. For the α-phase the LMF $\bar{f}$ and the center shift represent average values for the four different Cu-Zn configurations (see Sec. IV).

For both alloys the LMF decreases drastically with rising temperatures. All absorption lines move to more negative Doppler velocities. The four absorption lines of α-brass shift by the same amount within the experimental accuracy, the center shift of β'-brass is larger, in particular at 60 K. Except for this decrease in intensity and the shift to more negative velocities, the spectra do not change with temperature.

No transformation from the β'-phase to the α-phase, or vice versa, is observed.

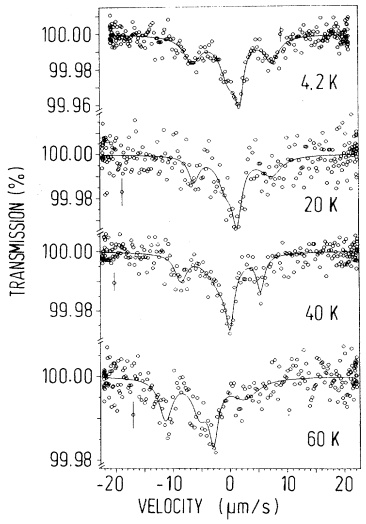

FIG. 1. ^{67}Zn Mössbauer absorption spectra of α-brass with 15.9 at.% Zn recorded at various temperatures. The source is ^{67}Ga in Cu metal.

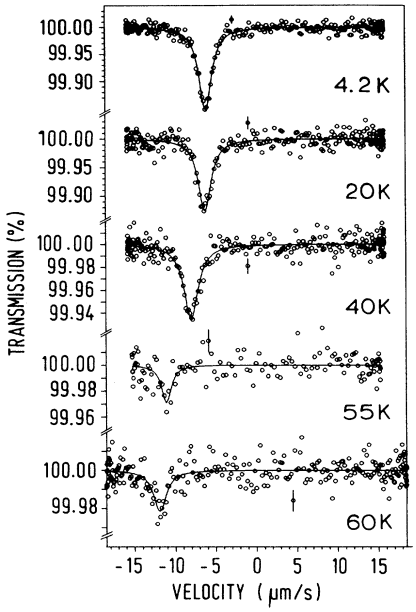

FIG. 2. ^{67}Zn Mössbauer absorption spectra of β'-brass with 49.2 at.% Zn recorded at various temperatures. The source is ^{67}Ga in Cu metal.

B. X-ray diffraction measurements

Figure 3 displays the volume changes of the α-alloy with 15.9 at.% Zn (a) and the β'-alloy with 49.2 at.% Zn (b) with temperature. The solid line represents a fit using the function

$$V(T) = \begin{cases} V_0\,(1 + u(T - T_0)) & \text{for } T \geq T_1 \\ bT^4 + c & \text{for } T \leq T_1, \end{cases} \quad (1)$$

where $T_0 = 298$ K, $V_0 = V(T_0)$, $b = (V_0 u)/(4T_1^3)$, $c = V_0(1 + u(0.75T_1 - T_0))$ and u is the thermal expansion coefficient at $T = T_0$. Equation (1) fulfills the criteria that for $T \to 0$ K the volume change should show a T^4 dependence and that for high temperatures the volume change is expected to be proportional to T.[15] The results are shown in Table V.

For the alloys containing 4.3 at.% Zn and 42.8 at.% Zn only the lattice parameters at room temperature have been determined (see Table V). The pressure dependence of the volume of the unit cell at room temperature has been determined earlier.[6] Unfortunately, only pressures up to ~10 GPa could be reached. Because of the strong correlation between the bulk modulus (B_0) and its pressure dependence (B_0') a unique determination of both values is impeded. From a comparison with other

TABLE I. Summary of Mössbauer parameters for α-brass with 15.9 at.% Zn at various temperatures T_A. The source is ^{67}Ga in Cu metal kept at temperature T_S. Only statistical errors are quoted for position, linewidth (full width at half maximum) and area (absorption depth × linewidth). The three upper sets of parameters (T_A=4.2 K, 20.0 K, and 40.0 K) refer to an absorber thickness of 0.194 g/cm^2 of ^{67}Zn, whereas the two lower sets (T_A=60.0 K, 4.2 K) are related to an increased absorber thickness of 0.382 g/cm^2. The last column gives the signal-to-background ratio in the 93.31-keV γ-ray window.

T_A (K)	T_S (K)	Position (μm/s)	Linewidth (μm/s)	Area (% μm/s)	$\frac{S}{S+B}$ (%)
4.2	4.2	−6.47(25)	3.58(87)	0.051(11)	61.2
		0.05(52)	3.7(1.0)	0.093(42)	
		1.83(13)	1.60(62)	0.044(28)	
		7.46(22)	3.05(73)	0.043(9)	
20.0(1)	7.97(28)	−6.26(37)	2.1(1.2)	0.024(12)	57.8
		−0.6(1.3)	3.4(2.7)	0.045(58)	
		1.32(29)	2.0(1.0)	0.054(46)	
		7.36(66)	4.3(2.2)	0.038(16)	
40.0(3)	12.9(1.5)	−8.60(24)	2.41(79)	0.021(6)	58.1
		−1.35(92)	5.7(1.4)	0.067(28)	
		0.02(13)	1.60(76)	0.027(20)	
		5.40(15)	1.59(52)	0.018(5)	
60.0(3)	19.1(4.1)	−11.35(22)	2.76(72)	0.027(6)	46.5
		−5.37(55)	3.1(1.7)	0.025(16)	
		−2.93(20)	1.97(78)	0.026(13)	
		2.54(79)	5.7(2.7)	0.028(12)	
4.2	4.2	−6.56(18)	3.21(62)	0.063(11)	43.0
		0.08(43)	4.0(1.0)	0.112(40)	
		1.918(84)	1.32(42)	0.043(21)	
		7.09(55)	7.4(1.7)	0.097(25)	

systems[6,16,17] we favor $B_0' \sim 4.3$ to derive $B_0 = 145$ GPa from the pressure data. Due to the uncertainty in B_0' we estimate an accuracy of ∼18% for B_0. Also the x-ray data give no indication of a phase transformation.

IV. DISCUSSION

A. Mössbauer measurements

1. α-brass

The Mössbauer spectrum of the α-brass alloy with 15.9 at.% Zn (see Fig. 1) shows only four absorption lines. Additional measurements on absorbers with Zn concentrations of 4.3, 10.0, and 24.6 at.% gave similar spectra:[18,5] Changing the Zn concentration (c_{Zn}) within the α-phase affects the relative intensities of the four lines but only very slightly their positions. Since the relative intensities change with c_{Zn} the absorption lines do *not* originate from quadrupole interactions. These observations are surprising and have been interpreted by the presence of short-range order, which gives rise to only four different Cu-Zn configurations in α-brass[18,5] instead of a binomial distribution expected from the high solubility of Zn in Cu. Such an analysis has recently been supported also by neutron diffraction experiments[7] and first-principles

TABLE II. Summary of Mössbauer parameters for β'-brass with 49.2 at.% Zn at various temperatures T_A. Symbols have the same meaning as in Table I.

T_A (K)	T_S (K)	Position (μm/s)	Linewidth (μm/s)	Area (% μm/s)	$\frac{S}{S+B}$ (%)
4.2	4.2	−6.101(24)	1.87(7)	0.286(8)	51.8
20.0(1)	7.86(20)	−6.227(41)	1.90(12)	0.241(12)	52.7
40.0(3)	13.5(2.3)	−7.975(53)	2.14(16)	0.139(8)	59.6
55.0(3)	17.4(1.8)	−11.04(13)	1.30(40)	0.040(9)	51.6
60.0(3)	20.1(3.7)	−11.94(13)	1.93(38)	0.041(6)	56.1

TABLE III. Summary of lattice-dynamical effects for α-brass with 15.9 at.% Zn at various temperatures T_A. The source is ^{67}Ga in Cu metal kept at temperature T_S. The average Lamb-Mössbauer factor (f) and the corresponding mean-square atomic displacements $\langle x^2 \rangle$ of ^{67}Zn are derived from the total absorption area taking the nonresonant background radiation $S/(S+B)$ and the Lamb-Mössbauer factor of the source into account. The three upper sets of parameters (T_A=4.2 K, 20.0 K, and 40.0 K) refer to an absorber thickness of 0.194 g/cm^2 of ^{67}Zn, whereas the two lower sets (T_A=60.0 K, 4.2 K) are related to an increased absorber thickness of 0.382 g/cm^2. The average center shift is given relative to its value at 4.2 K.

T_A (K)	T_S (K)	Average center shift (μm/s)	f (%)	$\langle x^2 \rangle$ (10^{-3} Å^2)
4.2	4.2		1.42(22)	$1.90(^{8}_{7})$
20.0(1)	7.97(28)	−0.26(24)	1.07(20)	$2.03(^{9}_{8})$
40.0(3)	12.9(1.5)	−1.93(14)	0.90(15)	$2.11(^{8}_{7})$
60.0(3)	19.1(4.1)	−4.90(18)	0.48(10)	$2.39(^{10}_{9})$
4.2	4.2		1.40(22)	$1.91(^{8}_{7})$

calculations.[8]

We will first discuss the Lamb-Mössbauer factor and the change of center shift with temperature under the assumption that lattice dynamical effects are the same for all four Cu-Zn configurations. In this way we can compare our results with one-phonon frequency distributions calculated from force constants models. Later we will relax this assumption and suggest the identification of Cu-Zn configurations from the line positions.

a. Lamb-Mössbauer factor (LMF). For pure Cu metal[19] as well as for the alloys Cu_3Zn (α-phase) (Ref. 20) and $Cu_{0.53}Zn_{0.47}$ (β'-phase) (Ref. 21) the phonon frequency distributions $\widetilde{Z}(\omega)$ have been determined earlier on the basis of phonon dispersion relations derived from inelastic neutron scattering data. In the case of Cu_3Zn model calculations were performed that included interactions up to the sixth-nearest-neighbor shell and allowed to determine 18 force constants between the atoms of the lattice. For the alloy $Cu_{0.53}Zn_{0.47}$ it was sufficient to take into account interactions up to the fourth-nearest-neighbor shell involving eight spring constants. The phonon frequency distributions of both alloys have to be modified slightly in order to represent the chemical compositions of our systems. This can be accomplished via the Lindemann formula[20,22] using well-known data for the melting points.[1] Concerning the variation of lattice constants with c_{Zn} within the α-phase a linear correlation is supported by published data[23,20] and our own measurements[24,29] (see Sec. III). We obtain $a = a_0 + bc_{Zn}$, where $a_0 = 3.61411$ Å is the lattice constant of Cu and $b = 2.25595 \times 10^{-3}$ Å/at.% Zn. The Lindemann formula results in a multiplication of the frequency axis of $\widetilde{Z}(\omega)$ of Cu_3Zn and of $Cu_{0.53}Zn_{0.47}$ by factors 1.023 and 0.990 to obtain $Z_\alpha(\omega)$ and $Z_{\beta'}(\omega)$, respectively, of our alloys. Figure 4 depicts these modified distributions together with $Z_{Cu}(\omega)$ of pure Cu metal.

Using $Z_{Cu}(\omega)$ we calculate for the LMF of pure Cu metal at 4.2 K f_{Cu}=2.06%, which is in good agreement with the results of a recent Mössbauer experiment, where we used ^{67}Ga in Cu metal as source and ^{67}ZnO as absorber. From the well-known lattice-dynamical properties of ^{67}ZnO (Ref. 25) we get f_S=2.0(2)% for the LMF of the ^{67}Ga*Cu* source at 4.2 K. During the measurements on the alloys at higher temperatures, the source temperature increased up to ~20 K (see Tables I–IV). The decrease of f_S as well as the change of the second-order Doppler shift (see below) in the source due to this rise in temperature was taken into account using $Z_{Cu}(\omega)$ when evaluating the Mössbauer data on the brass alloys. Within the Debye model, f_S=2.0% corresponds to an effective Debye temperature of Θ_D^{Cu}=310 K.

Assuming the LMF is the same for all four Cu-Zn configurations an average value $\overline{f}$ for LMF can be derived from the total area beneath the absorption lines after correction for nonresonant background radiation and using f_S=2.0(2)% at 4.2 K and its temperature varia-

TABLE IV. Summary of the center shift, the Lamb-Mössbauer factor (f) and the corresponding mean-square atomic displacement ($\langle x^2 \rangle$) of ^{67}Zn in β'-brass with 49.2 at.% Zn at various temperatures T_A. The source is ^{67}Ga in Cu kept at temperature T_S. Further details as in Table III.

T_A (K)	T_S (K)	Center shift (μm/s)	f (%)	$\langle x^2 \rangle$ (10^{-3} Å^2)
4.2	4.2		$0.80(^{14}_{11})$	2.16(7)
20.0(1)	7.86(20)	−0.128(48)	0.67(10)	2.24(7)
40.0(3)	13.5(2.3)	−1.887(59)	0.34(6)	$2.54(^{8}_{7})$
55.0(3)	17.4(1.8)	−4.98(13)	0.12(3)	$3.02(^{14}_{11})$
60.0(3)	20.1(3.7)	−5.91(14)	0.11(3)	$3.04(^{12}_{10})$

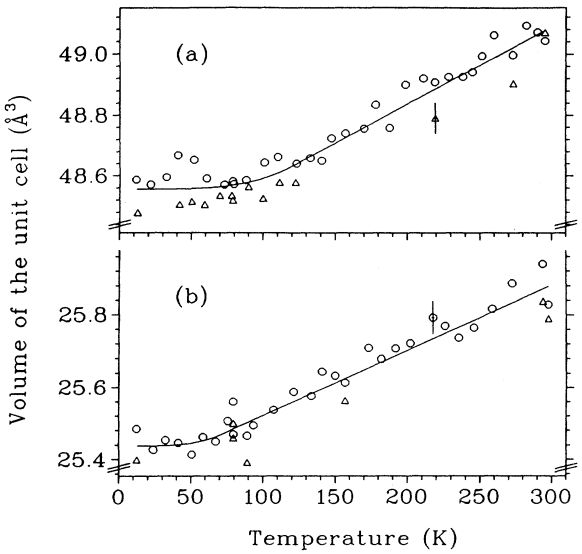

FIG. 3. Temperature dependence of the unit-cell volume for brass alloys with Zn concentrations of (a) 15.9 at.% and (b) 49.2 at.%. X-ray data were taken with a Guinier-type diffractometer.

tion just described. The temperature dependences of $\overline{f}$ and the corresponding mean-square atomic displacements $\langle x^2 \rangle$ for the α-phase is shown in Fig. 5.

Our results on $\overline{f}$ (and on $\langle x^2 \rangle$) can be described surprisingly well by the distribution $Z_\alpha(\omega)$. This is indicated by the solid line in Figs. 5. From $Z_\alpha(\omega)$ we calculate $\overline{f}$ = 1.58% at 4.2 K. The experimental values for $\overline{f}$ agree with the predictions obtained from $Z_\alpha(\omega)$ within ~10%, although $\overline{f}$ tends to be systematically lower. However, we would like to stress that the modification of $Z(\omega)$ via the Lindemann formula is only a crude approximation. If we start from $Z_{\mathrm{Cu}}(\omega)$ we calculate a multiplication factor of 0.962 for the composition of our α-alloy. This results in a recoil-free fraction of 1.77% as compared to 1.58%, given above. For this reason we argue that the systematic deviation is due to the presence of short-range order, which results in different Cu-Zn configurations. To apply the Lindemann formula we assumed, however, a homogeneous alloy with a binomial distribution of Zn in Cu.

For comparison, in Figs. 5 are also shown the results obtained by fitting the Debye model to our data. The effective Debye temperature of 285(2) K is in fair agreement with the effective Debye temperature of 302(3) K derived from specific-heat measurements (see Sec. IV A 1 *c*) but is much higher than Θ_D=249(2) K obtained for the β' alloy (see Sec. IV A 2).

b. Center shift. When the temperature is increased up to 60 K the relative intensities of the four absorption lines vary slightly (see below), the overall shape of the Mössbauer pattern remains virtually unchanged. The line positions, however, decrease towards more negative velocities. Within our experimental accuracy this change of center shift (CS) with temperature is the same for all four Cu-Zn configurations. At 60 K it amounts to −4.90(18) μm/s as shown in Fig. 6. The change of CS of α-brass (and, in particular, of the absorption line at ~−6.5 μm/s) is considerably smaller than of β'-brass (see Sec. IV A 2).

The experimental data on the CS are in very good agreement with the predicted second-order Doppler shift (SOD) derived from $Z_\alpha(\omega)$. Thus the CS is mainly due to SOD, a possible explicit temperature dependent isomer shift is negligibly small.

Also indicated in Fig. 6 are the variations according to the best fit to the Debye model. The effective Debye temperature of Θ_D=277(13) K agrees surprisingly well with Θ_D=285(2) K obtained from the LMF and its temperature dependence.

The different Cu-Zn configurations will now be addressed in more detail. The absorption line L_0 at ~0 μm/s (unshifted with respect to the emission line of the source) is to be identified with a configuration of one Zn atom surrounded by 12 nearest Cu neighbors, i.e., the same Cu-Zn configuration as in the source.[5,6] The absorption lines at positive velocities (~1.8 μm/s and ~7.5 μm/s) are caused by Cu-Zn configurations with more than one Zn atom in the nearest-neighbor shell.[5,6] For these configurations it is expected from theoretical calculations[26,27] that the *s*-electron density at the Zn nucleus is increased. These theoretical calculations show that *s*-electron transfer from Zn to Cu is important. More Zn atoms in the nearest-neighbor shell reduce this transfer effect per Zn atom, and thus the *s*-electron density $\rho(0)$ at the Zn nucleus in such configurations is increased. Within this model an absorption line at negative Doppler velocities cannot be accounted for and must be caused by a completely different mechanism, in particular, since the crystallographic structure is the same for the different Cu-Zn configurations. We argue that the absorption line L_1 at ~−6.5 μm/s is due to a highly stable Cu-

TABLE V. Summary of the results for the fit parameters used in Eq. (1). For the alloys with Zn concentrations c_{Zn} = 4.3 at.% and c_{Zn} = 42.8 at.% only the unit-cell volumes at room temperature have been determined.

c_{Zn} (at.% Zn)	V_0 (Å^3)	u (10^{-5} K^{-1})	b (10^{-10} Å^3 K^{-4})	c (Å^3)	T_1 (K)
4.3	47.458				
15.9	49.087(17)	5.21(32)	3.8(1.8)	48.6(2.4)	119(19)
42.8	50.309				
49.2	25.880(52)	6.90(33)	13.02(62)	25.44(54)	70 (fixed)

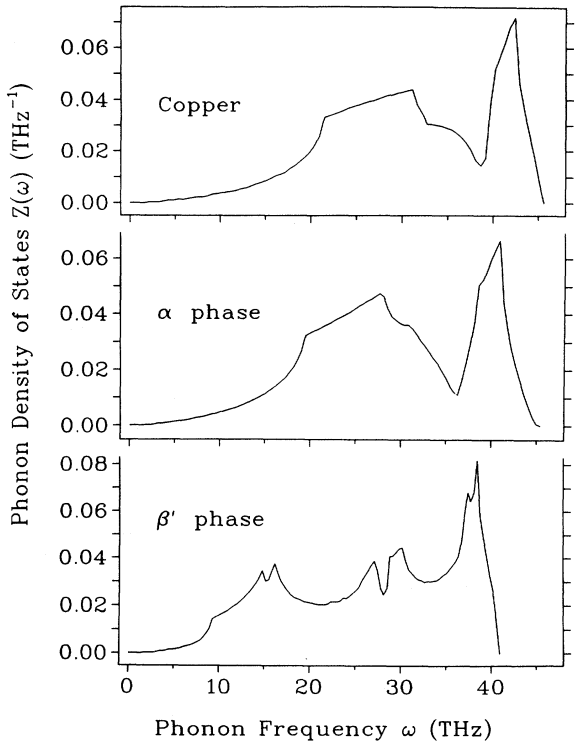

FIG. 4. Phonon frequency distributions for Cu metal [$Z_{Cu}(\omega)$] and the two brass alloys [$Z_\alpha(\omega)$, $Z_{\beta'}(\omega)$] investigated. These distributions were obtained from model calculations based on inelastic neutron scattering data. For details see text.

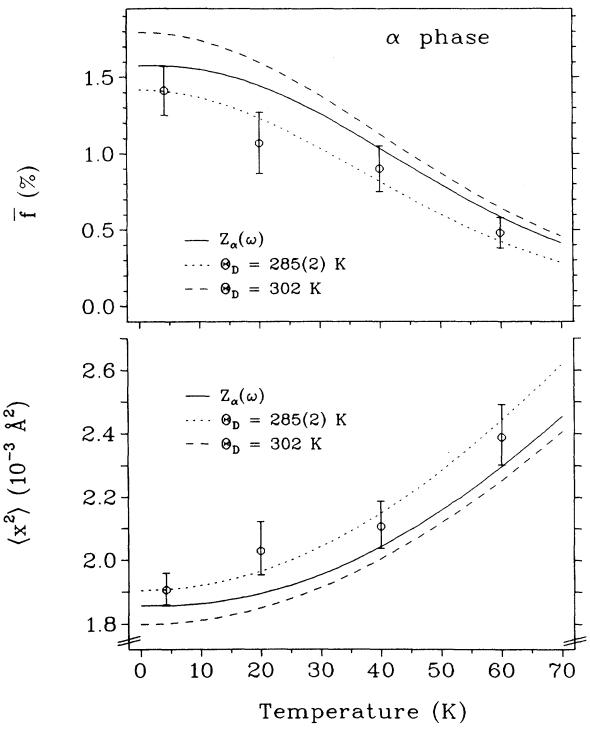

FIG. 5. Temperature dependence of the average Lamb-Mössbauer factor ($\bar{f}$) and of the average mean-square atomic displacements of ^{67}Zn in α-brass with 15.9 at.% Zn. Solid lines: Predictions obtained from $Z_\alpha(\omega)$. Dotted lines: Best fit to the Debye model. The dashed lines correspond to a Debye temperature Θ_D=302 K derived from specific-heat data of α-brass (see Fig. 7).

Zn configuration that exhibits stronger chemical bonds than the other configurations and gives rise to an absorption line at a negative Doppler velocity because of the second-order Doppler (SOD) shift. According to recent first-principles phase stability calculations[8] the most probable candidate is the Cu_3Zn configuration. In terms of the Debye model a SOD of -6.5 μm/s should correspond to an increase of the effective Debye temperature by $\Delta\Theta_D \sim 28$ K as compared to the configuration represented by the absorption line L_0. Such a difference in Θ_D should also manifest itself in the temperature behavior of the absorption areas (Table I). Unfortunately, our experimental accuracy is not sufficient to compare, for example, line L_1 with line L_0 directly. However, using the data of the 4.2 K and 60 K runs with the thick absorber, it is interesting to compare the ratio of areas of L_1 with the ratio of the sum of areas for the remaining three absorption lines. For L_1, the absorption area at 4.2 K is larger than at 60 K by a factor of $\sim$2.5, for the combined area of the other three lines the factor is $\sim$3.5. Within the Debye model the former gives an effective Debye temperature $\Theta_{\text{eff}}^{L_1} \sim 310$ K, the latter $\overline{\Theta}_{\text{eff}} \sim 280$ K, the difference being similar as $\Delta\Theta_D$ mentioned above. Furthermore, from $Z_\alpha(\omega)$ we calculate for the average LMF $\bar{f}$ =1.58% $\hat{=}$293 K, which falls right in between the values for $\Theta_{\text{eff}}^{L_1}$ and $\overline{\Theta}_{\text{eff}}$.

A difference of $\Delta\Theta_D \sim 28$ K should also result in a lower value for the temperature variation of CS between 4.2 K and 60 K of line L_1. Indeed, Fig. 6 shows that the variation of CS is compatible with effective Debye temperatures covering the range between 275 and 300 K. The formation of a highly stable configuration (e.g., Cu_3Zn) is consistent with our Mössbauer data.

When c_{Zn} is increased ($c_{Zn} \leq 16$ at.%) the positions of the absorption lines remain virtually unchanged (≤ 1 μm/s). This is due to two counteracting effects that nearly balance each other: Lattice expansion softens the phonon frequency spectrum, which causes a more positive SOD; on the other hand, the s-electron density $\rho(0)$ at the Zn nucleus is reduced (e.g., conduction electrons), which causes a more negative shift. This balance has also been observed in high-pressure experiments:[6] A volume change of $\sim$3% causes a shift of only $\sim$2 μm/s.

When c_{Zn} is increased, the average LMF is reduced because of the softening of the phonon frequencies and because more intensity is accumulated on lines at positive Doppler velocities. These absorption lines represent Cu-Zn configurations with more Zn and weaker bonds. Still, $Z_\alpha(\omega)$, which is based on neutron scattering data, provides a good description of the behavior of the average LMF and the average CS.

c. Specific heat. For α-brass with 19.77 at.% Zn specific-heat data C_P are also available.[28,29] To obtain

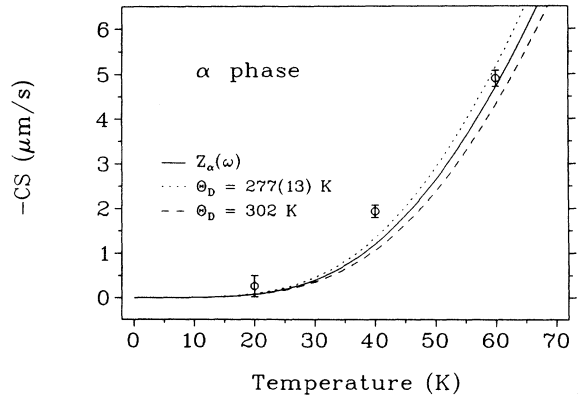

FIG. 6. Change of center shift (CS) of α-brass (15.9 at.% Zn) with temperature. Solid line: calculation of the second-order Doppler shift (SOD) using the phonon frequency distribution $Z_\alpha(\omega)$ derived from inelastic neutron scattering data. Dotted line: best fit to the Debye model [Θ_D=277(13) K]. Dashed line: Θ_D=302 K derived from specific-heat data.

the specific heat at constant volume (C_V) we have used the relation $C_P - C_V = V(T)T\,u^2(T)/\kappa_T$, where V is the molar volume, $\kappa_T = -1/V(T)[dV(T)/dp]_{T=\text{const}}$ is the isothermal compressibility at temperature T, and $u = 1/V(T)[dV(T)/dT]_{p=\text{const}}$ is the thermal expansion coefficient. The thermal expansion coefficient is derived from our x-ray measurements described above, the compressibility, $\kappa_T = 1/B_0 = 6.9(^{+1.2}_{-0.9}) \times 10^{-3}$ GPa^{-1} (see Sec. III). Figure 7 shows the experimental data together with the theoretical temperature dependence of C_V calculated from the appropriate phonon frequency distribution $Z_{\text{sp}}(\omega)$, which was obtained from $\bar{Z}(\omega)$ of Cu_3Zn after applying a Lindemann multiplication factor of 1.015 to take into account the chemical composition of this alloy. Considering the relatively large uncertainty in κ_T, the overall agreement with the experimental data is satisfactory. Still, as shown in the bottom part of Fig. 7, the experimental data are systematically lower also in the low-temperature regime, where the uncertainty of κ_T plays no role. We attribute this discrepancy—as in the case of the LMF—to the presence of short-range order effects, which are not taken into account properly neither by $Z_{\text{sp}}(\omega)$ nor by the Lindemann approximation.

A fit to the Debye model which gives Θ_D=302(3) K is also indicated. The effective Debye temperature is about 7% higher than the values derived from LMF and SOD. Nevertheless, this simple model describes all lattice-dynamical effects in α-brass surprisingly well.

2. β'-brass

a. Lamb-Mössbauer factor. Below ~725 K, β-brass forms an ordered alloy (β'-brass) with CsCl structure, i.e., each Zn atom is surrounded by eight Cu atoms. As expected for a cubic structure, the Mössbauer spectra recorded exhibit a single (rather narrow) Lorentzian line (see Fig. 2).

The temperature dependence of the LMF and the corresponding mean-square atomic displacement $\langle x^2\rangle$ for the β'-phase (49.2 at.% Zn) are shown in Fig. 8. The phonon frequency distribution $Z_{\beta'}(\omega)$ describes our results rather well. As in α-brass, the experimental values for the LMF are systematically smaller than the predictions calculated from $Z_{\beta'}(\omega)$. A fit of the Debye model to our data gives an effective Debye temperature of 249(2) K, which is considerably lower than Θ_D=285(2) K for the α-phase.

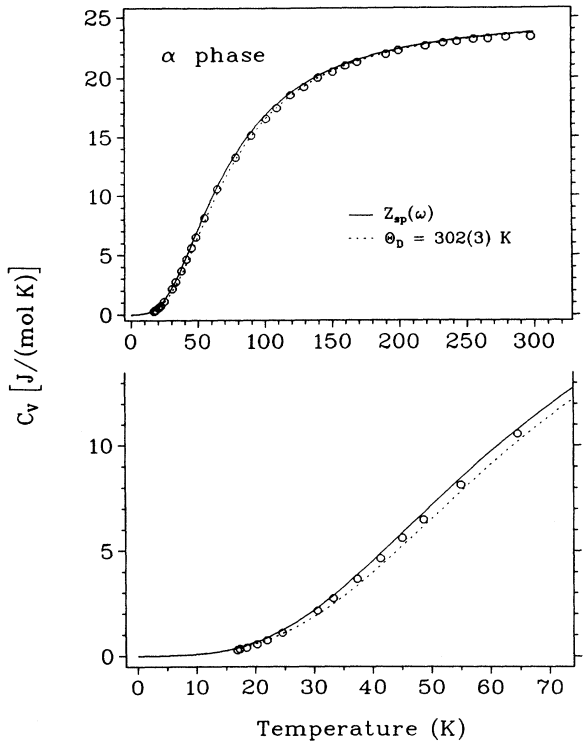

FIG. 7. Specific heat at constant volume (C_V) for α-brass containing 19.77 at.% Zn. The error bars for C_V are smaller than the symbols used for the data points. Solid line: Calculation using the phonon frequency distribution $Z_{\text{sp}}(\omega)$ derived from inelastic neutron-scattering data and slightly modified to represent the chemical composition of this alloy. Dotted line: Best fit to the Debye model with Θ_D=302(3) K. The bottom part of the figure gives an extended view of the temperature range up to 100 K.

b. Center shift. The position of the single absorption line of β'-brass (see Fig. 2) is shifted to negative velocities (~−6.1 μm/s) with respect to the source ^{67}Zn in fcc Cu, where each ^{67}Zn atom is surrounded by 12 Cu atoms in the nearest-neighbor shell. This shift cannot be caused by the second-order Doppler effect, since the phonon frequency spectrum of the source $Z_{\text{Cu}}(\omega)$ is harder than $Z_{\beta'}(\omega)$ for β'-brass, i.e., the effective Debye temperature of the source is higher than that for β'-brass. As a consequence, the s-electron density $\rho(0)$ at the ^{67}Zn nucleus has to be lower in β'-brass than at the highly diluted Zn sites in fcc Cu. Using $Z_{\text{Cu}}(\omega)$ and $Z_{\beta'}(\omega)$ we calculate for the second-order Doppler shift between the source and β'-brass 9.71 μm/s, which has to be subtracted from the CS of −6.1 μm/s. With $\Delta\langle r^2\rangle = 17.8\times10^{-3}$ fm^2

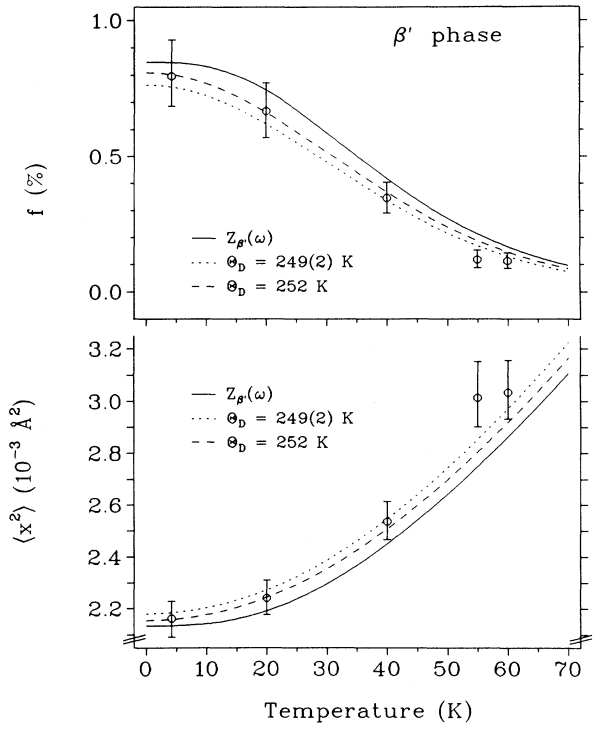

FIG. 8. Temperature dependence of the Lamb-Mössbauer factor (f) and of the mean-square atomic displacements of ^{67}Zn in β'-brass with 49.2 at.% Zn. Solid lines: Predictions obtained from $Z_{\beta'}(\omega)$. Dotted lines: Best fit to the Debye model. The dashed lines correspond to a Debye temperature Θ_D=252 K derived from the data on the second-order Doppler shift.

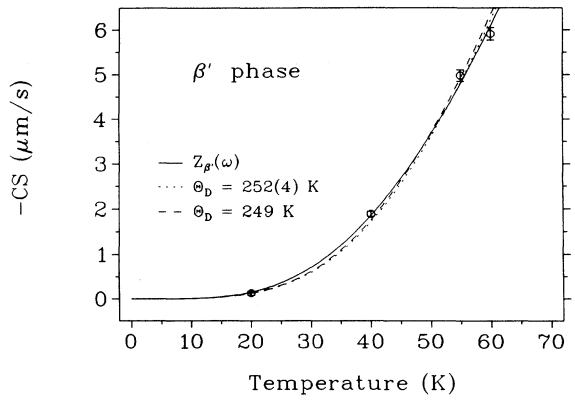

FIG. 9. Change of center shift (CS) of β'-brass (49.2 at.% Zn) with temperature. Solid line: Calculation of the second-order Doppler shift (SOD) using the phonon frequency distribution $Z_{\beta'}(\omega)$ derived from inelastic neutron scattering data. Dotted line: Best fit to the Debye model (Θ_D=252(4) K). Dashed line: Θ_D=249 K derived from data for the f-factor (see Fig. 8).

(Ref. 30) we obtain for the decrease $\Delta\rho(0)$ in contact density $\Delta\rho(0) = -0.45a_0^{-3}$, which is close to 16% of the total change in $\rho(0)$ between Zn metal and ZnO. The origin of the rather low contact density in the CsCl structure of β'-brass is not understood at present. It has been partially attributed to an increased shielding effect of the rather narrow 3d band of Zn in β'-brass as compared to α-brass.[31,32,18] Modern theoretical calculations[8,33,34] are called for to clarify the origin of this large decrease in $\rho(0)$.

When the temperature is raised to 60 K the CS of β'-brass decreases by 5.91(14) μm/s. This change of CS in β'-brass is considerably larger than that of the α-phase. Thus both, the data on the LMF as well as on the CS convincingly demonstrate that the absorption dip at $\sim$−6.5 μm/s in the α-alloy does not originate from β'-brass. A connection to β'-brass might have been surmised because of the very similar positions of the absorption lines, the comparable pressure dependence of their center shifts[6] and on the basis of a hypothetical phase diagram proposed recently.[9]

As exhibited in Fig. 9 the experimental data on the temperature variation of CS of β'-brass is in excellent agreement with the SOD calculated from $Z_{\beta'}(\omega)$. A Debye fit gives an effective Debye temperature Θ_D=252(4) K, which is in surprisingly good agreement with Θ_D=249(2) K obtained from the LMF and its temperature variation. An upper limit for an explicit temperature-dependent isomer shift can be estimated from the volume increase due to thermal expansion at 60 K and from the volume dependence of the isomer shift determined earlier.[6] We get −0.12(2) μm/s, which is only $\sim$2% of the observed CS. Thus, similar to α-brass, the CS is almost completely due to SOD in the temperature regime up to 60 K.

B. X-ray diffraction measurements

Our data on the unit-cell volume for α- and β'-brass at room temperature are in good agreement with results given in the literature.[35,36] This also holds for the thermal expansion coefficient for the α-alloy, where we get u_α(298 K)= (5.21 ± 0.32) × 10^{-5} K^{-1}, which can be compared with u_α(293 K)= 5.25 × 10^{-5} K^{-1} given in Ref. 37.

For α-brass the Grüneisenparameter $\gamma = u(T)V(T)/[\kappa_T C_V(T)]$ can be calculated from the thermal expansion coefficient, the unit-cell volume, the compressibility and the specific-heat data. In the low-temperature limit we get γ(4.2 K)$\sim$ 0.5 and at high temperatures γ(298 K) $\sim$ 2.8. Both values are much smaller than $\tilde{\gamma}$(4.2 K)$\sim$ 4.9 derived from the increase in LMF in high-pressure Mössbauer experiments at 4.2 K.[6] This discrepancy is not understood at present. A similar situation has been found for Zn metal under high external pressure.[38]

V. CONCLUSIONS

The temperature dependence of the LMF and of the SOD derived from Mössbauer experiments on α- and β'-brass alloys as well as low-temperature x-ray measurements demonstrate that no β'-phase is present in the α-

alloy contrary to the prediction of a hypothetical phase diagram proposed recently.[9]

The absorption line at ~ -6.5 μm/s in α-brass is most probably caused by the highly stable Cu_3Zn configuration and is shifted to this negative Doppler velocity because of the large second-order Doppler effect. The absorption line in β'-brass, however, is shifted to a negative velocity (-6.1 μm/s) because of a considerable reduction of the s-electron density $\rho(0)$ at the Zn nucleus. The origin of this decrease in $\rho(0)$ is not yet understood.

The variations of LMF and SOD with temperature of both alloys can well be described by the phonon frequency distributions, which are obtained from detailed model calculations based on inelastic neutron scattering data. The explicit temperature dependence of the isomer shift is negligible up to 60 K, the highest temperature reached in this investigation. Although the effective Debye temperatures as determined from LMF, SOD, and specific-heat data differ slightly within each alloy this simple model describes all lattice-dynamical effects surprisingly well. This is probably due to the highly symmetric (cubic) crystallographic structures of both alloys and the rather small difference in masses between Cu and Zn.

ACKNOWLEDGMENTS

We would like to thank the Kernforschungszentrum Karlsruhe, especially Dr. H. Schweickert, K. Assmus, and W. Maier for numerous and careful source irradiations at the cyclotron. This work has been funded by the German Federal Minister for Research and Technology [Bundesminister für Forschung und Technologie (BMFT)] under Contract No. 03-KA2TUM-4 and by the Kernforschungszentrum Karlsruhe.

[1] M. Hansen and K. Anderko, *Constitution of Binary Alloys* (McGraw-Hill, New York, 1958), p. 650; R. P. Elliott, *Constitution of Binary Alloys*, 1st Suppl. (McGraw-Hill, New York, 1965), p. 390; C. J. Smithells, *Metals Reference Book*, 4th ed. (Butterworths, London, 1967), Vol. II.

[2] W. Hume-Rothery, J. Instrum. Methods **35**, 307 (1926).

[3] V. Heine and D. Weaire, in *Solid State Physics*, edited by H. Ehrenreich, F. Seitz, and D. Turnbull (Academic, New York, 1970), Vol. 24, p. 249.

[4] T. B. Massalski and U. Mizutani, Prog. Mater. Sci. **22**, 151 (1978).

[5] Th. Obenhuber, W. Adlassnig, U. Närger, J. Zänkert, W. Potzel, and G. M. Kalvius, Europhys. Lett. **3**, 989 (1987).

[6] W. Adlassnig, W. Potzel, J. Moser, W. Schiessl, U. Potzel, C. Schäfer, M. Steiner, H. Karzel, M. Peter, and G. M. Kalvius, Phys. Rev. B **40**, 7469 (1989), and references therein.

[7] L. Reinhard, B. Schönfeld, G. Kostorz, and W. Bührer, Phys. Rev. B **41**, 1727 (1990).

[8] P. E. A. Turchi, M. Sluiter, F. J. Pinski, D. D. Johnson, D. M. Nicholson, G. M. Stocks, and J. B. Staunton, Phys. Rev. Lett. **67**, 1779 (1991).

[9] E. Hornbogen, Z. Metallkde. **78**, 689 (1987).

[10] M. Steiner, W. Potzel, C. Schäfer, W. Adlassnig, M. Peter, H. Karzel, and G. M. Kalvius, Phys. Rev. B **41**, 1750 (1990), and references therein.

[11] W. Potzel, Th. Obenhuber, A. Forster, and G. M. Kalvius, Hyperfine Interact. **12**, 135 (1982).

[12] W. Potzel and N. Halder, Nucl. Instrum. Methods. **226**, 418 (1984).

[13] W. Potzel, High Pressure Research **2**, 367 (1990).

[14] H. Karzel, U. Potzel, W. Potzel, J. Moser, C. Schäfer, M. Steiner, M. Peter, A. Kratzer, and G. M. Kalvius, Mater. Sci. Forum **79-82**, 419 (1991).

[15] G. Leibfried and W. Ludwig, in *Solid State Physics*, edited by F. Seitz and D. Turnbull (Academic, New York, 1961), Vol. 12, p. 275.

[16] J. A. Moriarty, Phys. Rev. B **45**, 2004 (1992).

[17] K. W. Katahara, M. H. Manghnani, and E. S. Fisher, J. Phys. F **9**, 773 (1979).

[18] Th. Obenhuber, W. Adlassnig, J. Zänkert, U. Närger, W. Potzel, and G. M. Kalvius, Hyperfine Interact. **33**, 69 (1987).

[19] R. M. Nicklow, G. Gilat, H. G. Smith, L. J. Raubenheimer, and M. K. Wilkinson, Phys. Rev. **164**, 922 (1967).

[20] E. D. Hallmann and B. N. Brockhouse, Can. J. Phys. **47**, 1117 (1969).

[21] G. Dolling and G. Gillat, in *Inelastic Scattering of Neutrons* (IAEA, Vienna, 1965), Vol. 1, p. 343.

[22] J. A. Reissland, in *The Physics of Phonons* (Wiley, London, 1973).

[23] S. S. Rao and T. R. Anantharaman, Current Sci. (India) **32**, 262 (1963); L. H. Beck and C. S. Smith, J. Metals **4**, 1079 (1952); E. A. Owen and L. Pickup, Proc. R. Soc. London Ser. A **145**, 258 (1934); Strukturberichte **3**, 593 (1937).

[24] J. P. Zänkert, Ph.D. thesis, Technische Universität München, 1985; W. Schiessl, Diploma thesis, Technische Universität München, 1989.

[25] C. Schäfer, W. Potzel, W. Adlassnig, P. Pöttig, E. Ikonen, and G. M. Kalvius, Phys. Rev. B **37**, 7247 (1988).

[26] A. Bansil, H. Ehrenreich, L. Schwartz, and R. E. Watson, Phys. Rev. B **9**, 445 (1974).

[27] R. Prasad and A. Bansil, Phys. Rev. Lett. **48**, 113 (1982), and references therein.

[28] Y. S. Touloukian and E. H. Buyco, *Thermophysical Properties of Matter* (IFI/Plenum, New York, 1970), Vol. 4, p. 346.

[29] M. Peter, Diploma thesis, Technische Universität München, 1990.

[30] F. Buheitel, W. Potzel, and D. C. Aumann, Hyperfine Interact. **47-48**, 606 (1989).

[31] G. K. Wertheim, M. Campagna, and S. Hüfner, Phys. Condens. Matter **18**, 133 (1974).

[32] Th. Obenhuber, W. Adlassnig, J. Zänkert, U. Närger, W. Potzel, and G. M. Kalvius, Hyperfine Interact. **28**, 1033 (1986).

[33] H. H. Klauss, N. Sahoo, P. C. Kelires, T. P. Das, W. Potzel, G. M. Kalvius, M. Frank, and W. Kreische, Hyperfine Interact. **60**, 853 (1990).

[34] D. W. Mitchell, S. B. Sulaiman, N. Sahoo, T. P. Das, W.

Potzel, and G. M. Kalvius, Phys. Rev. B **44**, 6728 (1991).
[35]V. Göhler and G. Sachs, Z. Phys. **55**, 618 (1929).
[36]E. A. Owen and L. Pickup, Proc. R. Soc. London, Ser. A **145**, 258 (1934).
[37]Y. S. Touloukian, R. K. Kirby, R. E. Taylor, and P. D. Desai, *Thermophysical Properties of Matter* (IFI/Plenum, New York, 1975), Vol. 12, p. 797.
[38]W. Potzel, W. Adlassnig, J. Moser, C. Schäfer, M. Steiner, and G. M. Kalvius, Phys. Rev. B **39**, 8236 (1989).